

A Novel Low-Bandgap Conjugated Polymer Based on Ru(II) Bis(acetylide) Complex and BODIPY Moieties

Shuwei Zhang, Yuan Sheng, Guo Wei, Yiwu Quan, Yixiang Cheng, Chengjian Zhu

Key Lab of Mesoscopic Chemistry of MOE, School of Chemistry and Chemical Engineering, Nanjing University, Nanjing 210093, China

Correspondence to: Y. Cheng (E-mail: yxcheng@nju.edu.cn) or C. Zhu (E-mail: cjzhu@nju.edu.cn)

Received 13 November 2013; accepted 11 March 2014; published online 1 April 2014

DOI: 10.1002/pola.27166

ABSTRACT: A novel conjugated polymer **P-1** incorporating Ru(II) bis(acetylide) complex and borondipyrromethene (BODIPY) moieties in the main chain was synthesized by Pd-catalyzed Sonogashira coupling reaction of diethynyl substituted BODIPY derivative (**M-1**) and Ru(II) bis(acetylide) complex (**M-2**), and the reference polymer **P-2** was obtained from the same method as preparation of **P-1**. Compared with **P-2**, Ru(II)-containing polymer **P-1** shows low-bandgap as 0.87 eV from cyclic voltam-

metry, and obvious redshifts in both UV-vis absorption and fluorescence spectra. © 2014 Wiley Periodicals, Inc. *J. Polym. Sci., Part A: Polym. Chem.* **2014**, *52*, 1686–1692

KEYWORDS: BODIPY; conjugated polymers; electrochemistry; heteroatom-containing polymers; low-bandgap; Ru(II) bis(acetylide) complex

INTRODUCTION Conjugated polymers (CPs) containing transition metals in the backbone have been studied extensively for chemical sensors, electroluminescent devices, field-effect transistors, solar cells, and so on, due to their special redox, magnetic, and electrical properties.^{1–6} For instance, some CPs incorporating Ir(III) and Ru(II) complexes show efficient phosphorescent emission and could be used for organic light-emitting diodes (OLED).^{7–10} Among these materials, rigid-rod organometallic CPs, which contain transition metal fragments linked with acetylenic chromophores in the polymer main backbone, have attracted increasing interests, because this special structure could result in beneficial influence on extended $d-\pi$ conjugation and electronic properties of the CPs.^{11–13} Wong et al. reported bulk heterojunction (BHJ) solar cells incorporating thiophene-based polyplatinynes with power conversion efficiencies (PCEs) as high as 4.1%.¹⁴ Besides platinum complexes, other transition-metal complexes, especially Ru(II) complexes, also exhibit special optical and electrical properties due to the rich electronic structures of their metal centers and organic ligands.^{15–17} Some of them have been introduced into the polymer backbones to realize the desirable optoelectronic materials.^{18,19}

Over the past decades, 4,4-difluoro-4-bora-3a,4a-diaza-s-indacene (BODIPY) and its derivatives have become one of the versatile fluorophores due to their good optical properties, such as high absorption coefficients, narrow absorption band, and high quantum yields, and so forth.^{20–24} And

BODIPY-based CPs have been extensively studied for fluorescent sensors, dye-sensitized solar cells, and so on.^{25–28} Recently, several groups have researched BODIPY-based transition-metal complexes.^{29–31} However, to the best of our knowledge, all of them are based on small molecules. There has been no report on BODIPY-based CPs containing transition-metal complexes.

Herein, to investigate a kind of novel materials with low-bandgaps and broad absorption in visible to near-infrared regions, we designed and synthesized a BODIPY-based and Ru(II) complex-containing CP **P-1**, which could effectively tune the electronic properties by introduction of Ru(II) complex moieties in the polymer main backbone. As expected, compared with the reference polymer **P-2** without Ru(II) complex moieties, the bandgap of **P-1** can be greatly decreased from 1.51 to 0.87 eV.

EXPERIMENTAL

Materials and Measurements

All solvents and reagents were commercially available and analytical reagent grade. THF and Et₃N were distilled from sodium in the presence of benzophenone. NMR spectra were obtained from Bruker Avance 300 spectrometer with 300 MHz for ¹H NMR and 75 MHz for ¹³C NMR, Bruker DRX 400 spectrometer with 162 MHz for ³¹P NMR, and Bruker DRX 500 spectrometer with 160 MHz for ¹¹B NMR. UV-vis spectra were obtained from a Perkin-Elmer Lambda 25

Additional Supporting Information may be found in the online version of this article.

© 2014 Wiley Periodicals, Inc.

spectrometer. Fluorescence spectra were obtained from a RF-5301PC spectrometer. Time-resolved fluorescence decays were obtained from HORIBA JOBIN YVON Tem Pro-01 lifetime fluorescence spectroscopy. Electrospray ionization mass spectra (ESI-MS) were obtained from a Thermo Finnigan LCQ Fleet system. FTIR spectra were measured on a Nexus 870 FTIR spectrometer. Elemental analyses were performed on an Elementar Vario MICRO analyzer. Thermogravimetric analyses (TGA) were obtained from a Perkin-Elmer Pyris-1 instrument under N₂ atmosphere. Molecular weight was determined by gel permeation chromatography (GPC) with a Waters 244 HPLC pump, and THF was used as solvent relative to polystyrene standards.

Synthesis of M-1

A mixture of **2** (1.0 g, 1.42 mmol), Pd(PPh₃)₂Cl₂ (49.8 mg, 5% mmol), CuI (27.0 mg, 10% mmol) were dissolved in anhydrous THF (20 mL), then trimethylsilylacetylene (726 mg, 4.26 mmol) in THF (5 mL) and Et₃N (5 mL) was added under N₂ atmosphere. The reaction mixture was stirred for 24 h at 50 °C. Then the solvent was removed under reduced pressure to afford the residue. The residue was dissolved in MeOH (50 mL), then K₂CO₃ (0.58 g, 4.20 mmol) was added. The reaction mixture was stirred for 3 h at room temperature. Then the reaction mixture was filtrated, and the filtrate was concentrated to afford the residue. The residue was dissolved in CH₂Cl₂ (60 mL), and the organic solution was washed with water and brine, then dried over anhydrous Na₂SO₄. After filtration, the solvent was removed to afford crude product. The crude product was purified by silica gel chromatography (petroleum ether/ethyl acetate, vol/vol, 10/ 1) to afford **M-1** (0.52 g, 72.6%) as a deep red solid. ¹H NMR (300 MHz, CDCl₃): δ 7.50–7.44 (m, 1H), 7.12–7.09 (m, 2H), 7.01 (d, *J* = 9.0 Hz, 1H), 3.97 (t, *J* = 7.5 Hz, 2H), 3.32 (s, 2H), 2.67 (s, 6H), 1.65–1.61 (m, 2H), 1.55 (s, 6H), 1.31–1.18 (m, 10H), 0.88 (t, *J* = 7.5 Hz, 3H); ¹³C NMR(75 MHz, CDCl₃): δ 158.1, 155.7, 144.9, 140.9, 131.0, 129.1, 123.2, 121.3, 114.6, 112.3, 83.7, 76.0, 68.4, 31.6, 29.6, 29.2, 29.1, 28.8, 25.8, 22.6, 14.0, 13.4, 12.6; MS (ESI): *m/z* calcd for C₃₁H₃₅BF₂N₂O: 500.28 [M⁺]; found: 501.30.

Synthesis of M-2

A mixture of **4** (360 mg, 0.97 mmol) and Et₃N (0.3 mL) in CH₂Cl₂ (20 mL) was added to **3** (315 mg, 0.33 mmol) and KPF₆ (195 mg, 0.97 mmol) in CH₂Cl₂ (10 mL). The reaction was stirred for 40 h at room temperature. After filtration, the filtrate was concentrated to afford the residue. Then the residue was washed with hexane, water, and ethanol consecutively to afford 315 mg crude product as a deep yellow solid. The crude product was recrystallized in hexane/CH₂Cl₂ to afford **M-2** (280 mg, 52.5%) as a yellow solid. ¹H NMR (300 MHz, CDCl₃): δ 7.48–7.46 (m, 16H), 7.23 (s, 2H), 7.12–7.07 (m, 8H), 6.89–6.84 (m, 16H), 5.74 (s, 2H), 3.90 (t, *J* = 6.0 Hz, 4H), 3.67 (t, *J* = 6.0 Hz, 4H), 2.91 (s, 8H), 1.79–1.30 (m, 16H), 1.00 (t, *J* = 7.5 Hz, 6H), 0.86 (t, *J* = 7.5 Hz, 6H); ³¹P NMR (162 MHz, CDCl₃): δ 44.99; FTIR (KBr, cm⁻¹): 2048 (νCCRu); ELEM. ANAL. calcd (%) for C₈₄H₈₈I₂O₄.

P₄Ru: C 61.50, H 5.41; Found: C 62.05; H 5.49; MS (ESI): *m/z* calcd for C₈₄H₈₈I₂O₄P₄Ru: 1640.28 [M⁺]; found: 1640.50.

Synthesis of M-3

A mixture of **4** (500 mg, 1.34 mmol), *N,N,N',N'*-tetramethylethylenediamine (TMEDA) (0.05 mL, 0.27 mmol), CuI (12.8 mg, 0.07 mmol), and Et₃N (0.56 mL, 4.02 mmol) were added to acetone (15 mL). The reaction was stirred for 16 h at room temperature. The product was formed as precipitation. After filtration, the solid was dissolved in CH₂Cl₂ (100 mL). And the organic solution was washed with water and brine, dried over anhydrous Na₂SO₄. After filtration, the solvent was removed to afford **M-3** (320 mg, 64.3%) as a yellow solid. ¹H NMR (300 MHz, CDCl₃): δ 7.31 (s, 2H), 6.90 (s, 2H), 4.02–3.94 (m, 8H), 1.86–1.77 (m, 8H), 1.62–1.48 (m, 8H), 1.03–0.98 (m, 12H); ¹³C NMR(75 MHz, CDCl₃): δ 155.5, 151.7, 123.8, 116.5, 112.1, 89.0, 78.7, 78.4, 69.7, 69.6, 31.1, 19.2, 19.1, 13.7; MS (ESI): *m/z* calcd for C₃₂H₄₀I₂O₄: 765.09 [M+Na⁺]; found: 765.05.

Synthesis of Reference Compound 6

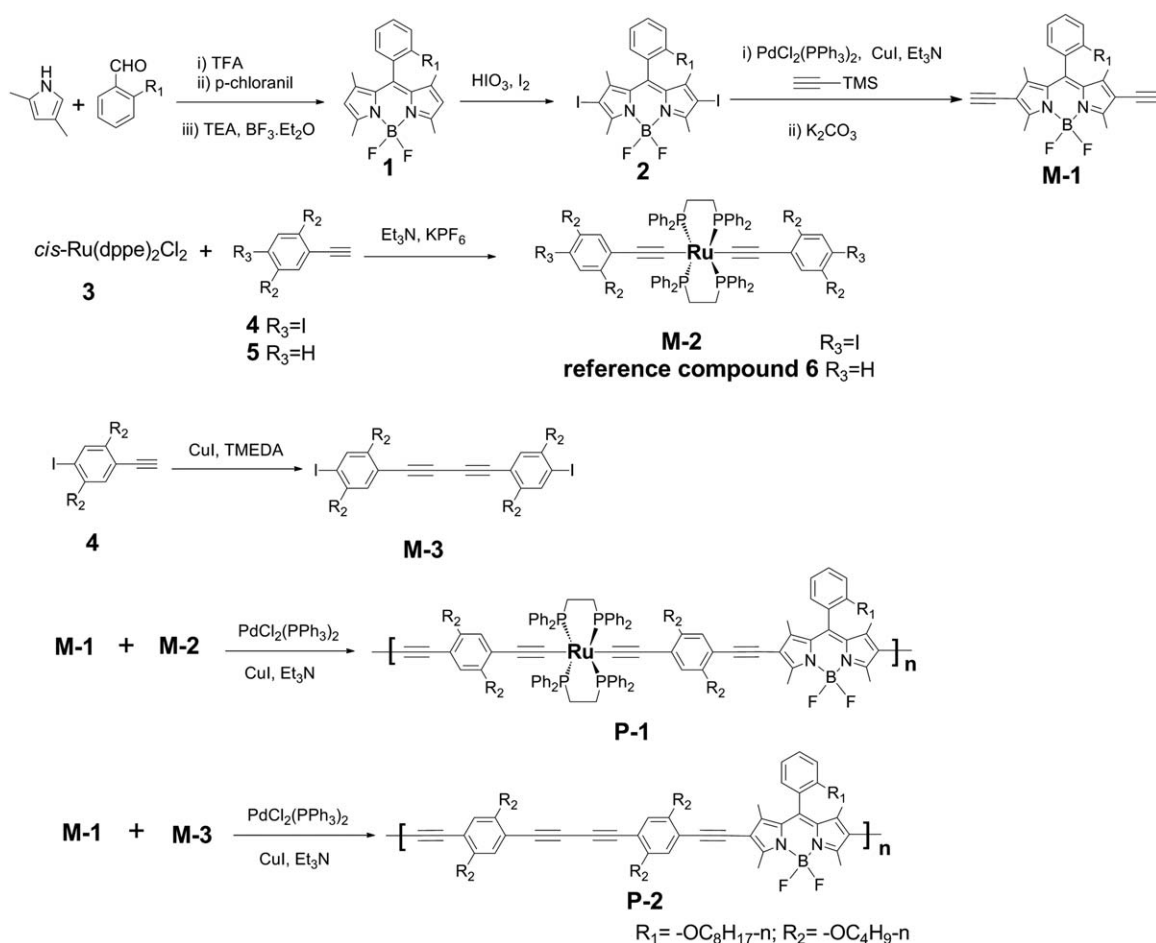
Compound 6 was synthesized from **3** and **5** by following the same procedure as preparation of **M-2**. ¹H NMR (300 MHz, CDCl₃): δ 7.53–7.50 (m, 16H), 7.11–7.06 (m, 8H), 6.90–6.85 (m, 16H), 6.77 (d, *J* = 9.0 Hz, 2H), 6.49 (brs, 2H), 5.97 (s, 2H), 3.87 (t, *J* = 6.0 Hz, 4H), 3.74 (t, *J* = 6.0 Hz, 4H), 2.92 (s, 8H), 1.78–1.59 (m, 8H), 1.54–1.29 (m, 8H), 1.00 (t, *J* = 7.5 Hz, 6H), 0.85 (t, *J* = 7.5 Hz, 6H); ³¹P NMR (162 MHz, CDCl₃): δ 48.51; FTIR (KBr, cm⁻¹): 2051 (νCCRu); ELEM. ANAL. calcd (%) for C₈₄H₉₀O₄P₄Ru: C 72.66, H 6.53; Found: C 72.28, H 6.61; MS (ESI): *m/z* calcd for C₈₄H₉₀O₄P₄Ru: 1388.48 [M⁺]; found: 1388.55.

Synthesis of P-1

A mixture of **M-1** (48.6 mg, 0.097 mmol), **M-2** (160 mg, 0.097 mmol), Pd(PPh₃)₄ (5.6 mg, 5% mmol), CuI (1.88 mg, 10% mmol) were added to THF (10 mL) and Et₃N (5 mL) under N₂ atmosphere. The reaction was stirred at 40 °C for 40 h. Then the mixture was cooled to room temperature and filtrated through a short silica gel column. Then the polymer was precipitated in methanol (100 mL). The polymer was filtrated and washed with methanol several times. Further purification could be conducted by dissolving the polymer in CH₂Cl₂ to precipitate in methanol again. The polymer was dried in vacuum to afford **P-1** (140 mg, 76.2%) as a deep blue solid. GPC results: *M_w* = 12,050, *M_n* = 7440, polydispersity index (PDI) = 1.62; ¹H NMR (300 MHz, CDCl₃): δ 7.47–7.45 (br, 17H), 7.12 (s, 2H), 7.11–7.07 (m, 10H), 6.93–6.84 (m, 17H), 5.87–5.79 (m, 2H), 3.99–3.84 (m, 6H), 3.68–3.60 (m, 4H), 2.91–2.68 (m, 14H), 1.79–1.17 (m, 34H), 1.02–0.83 (m, 15H); FTIR(KBr, cm⁻¹): 2928, 2869, 2192, 2048, 1525, 1485, 1466, 1312, 1189, 1010, 695, 530; ELEM. ANAL. calcd (%) for C₁₁₅H₁₂₃BF₂N₂O₅P₄Ru: C 73.20, H 6.57; Found: C 71.62, H 6.03.

Synthesis of P-2

A mixture of **M-1** (80 mg, 0.160 mmol), **M-3** (118.7 mg, 0.160 mmol), Pd(PPh₃)₄ (9.2 mg, 5% mmol), CuI (3.04 mg,



SCHEME 1 Synthesis of monomers and polymers.

10% mmol) was dissolved in THF (10 mL) and Et₃N (5 mL) under N₂ atmosphere. The reaction mixture was stirred for 40 h at 40 °C. Then the mixture was cooled to room temperature and filtrated through a short silica gel column. Then the polymer was precipitated in methanol (100 mL). The polymer was filtrated and washed with methanol several times. Further purification could be conducted by dissolving the polymer in CH₂Cl₂ to precipitate in methanol again. The polymer was dried in vacuum to afford **P-2** (132 mg, 83.2%) as a deep red solid. GPC results: $M_w = 15,980$, $M_n = 10,380$, PDI = 1.54; ¹H NMR (300 MHz, CDCl₃): δ 7.60–7.54 (m, 1H), 7.18–7.11 (m, 2H), 7.04–7.00 (m, 1H), 6.96 (s, 2H), 6.90 (s, 2H), 4.03–3.94 (m, 10H), 2.76–2.69 (m, 6H), 1.84–1.72 (m, 8H), 1.64–1.44 (m, 16H), 1.28–1.19 (m, 10H), 1.03–0.92 (m, 12H), 0.88–0.80 (m, 3H); FTIR(KBr, cm⁻¹): 2928, 2870, 2200, 2138, 1532, 1491, 1468, 1316, 1184, 1012, 713, 584; ELEM. ANAL. calcd (%) for C₆₃H₇₅BF₂N₂O₅: C 76.50, H 7.64; Found: C 74.69, H 6.22.

RESULTS AND DISCUSSION

Synthesis and Structural Characterization

The synthetic routes to the monomers and polymers are shown in Scheme 1. BODIPY derivatives (**1**, **2**),^{32,33} *cis*-

[Ru(dppe)₂Cl₂] (**3**),^{34,35} 1,4-dibutoxy-2-ethynyl-5-iodobenzene (**4**),³⁶ and 1,4-dibutoxy-2-ethynylbenzene (**5**)³⁷ were prepared according to reported literatures. **M-1** was synthesized by Pd-catalyzed Sonogashira coupling reaction of compound **2** and trimethylsilylacetylene, **M-2** and reference compound **6** were synthesized by the dehydrohalogenation reaction from compound **3** and **4** or **5**.^{38,39} 1,4-Bis(2,5-dibutoxy-4-iodophenyl)buta-1,3-diyne (**M-3**) was prepared by Cu-catalyzed oxidative coupling reaction from the compound **4** in a moderate yield of 64.3%.^{40,41} **P-1** and **P-2** were synthesized by Pd-catalyzed Sonogashira coupling reaction from **M-1** and **M-2** or **M-3** in yields of 76.2 and 83.2%, respectively. The chemical structures of the polymers could be confirmed by ¹H NMR and IR spectroscopies. Compared with the ¹H NMR spectra of monomers, the two polymers have the related proton signals, and no peaks at about 3.3 ppm where acetylene protons resonate. Meanwhile, the IR spectrum of **P-1** and **P-2** also show no absorption bands at about 3300 cm⁻¹ which are assignable to the stretching vibrations of ≡CH. This demonstrates the successful preparation of the target polymers. The resulting polymers show excellent solubility in common organic solvents. The number average molecular weight and PDI of the polymers measured by GPC were $M_n = 7440$ and PDI = 1.62 for **P-1**, $M_n = 10,380$ and PDI = 1.54 for **P-2**.

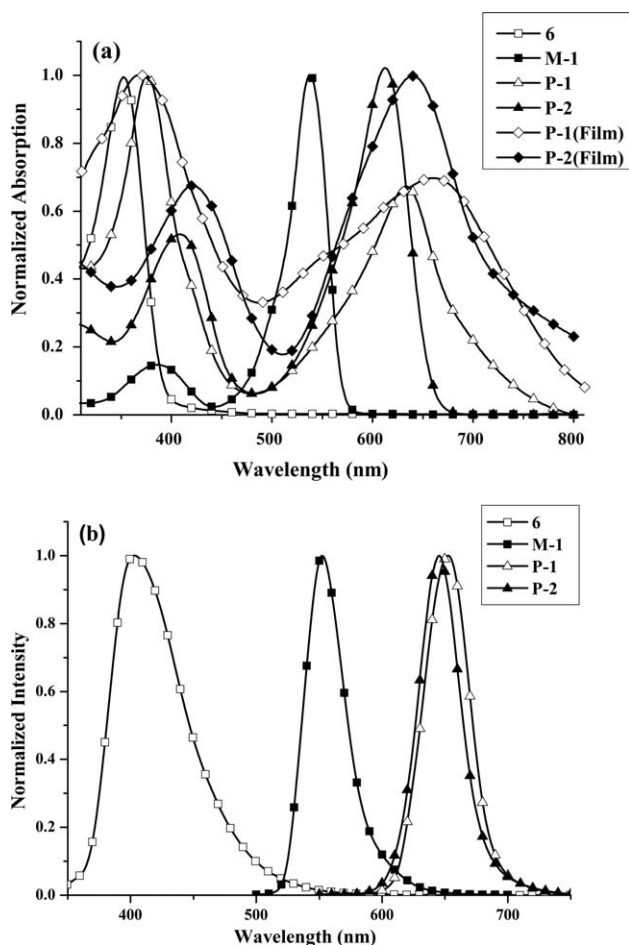


FIGURE 1 (a) Normalized UV-vis absorption spectra in CH_2Cl_2 solutions and solid films and (b) Normalized emission spectra in CH_2Cl_2 solutions of **6**, **M-1**, **P-1**, **P-2**.

The TGA curves (Supporting Information Fig. S18) reveal that the degradation temperature (T_d) of 5% weight loss of **P-1** and **P-2** are 269 and 268 °C, respectively, which indicates an excellent thermal stability of the polymers.

Optical Properties

The UV-vis absorption and fluorescence spectra of the polymers, **M-1** and reference compound **6**, are shown in

Figure 1, and the corresponding optical data is listed in Table 1. As shown in UV-vis absorption spectra [Fig. 1(a)] measured in solutions, **M-1** appears as a strong $S_0 \rightarrow S_1$ ($\pi-\pi^*$) transition at 538 nm and a much weaker broad band at a shorter wavelength 388 nm probably ascribing to $S_0 \rightarrow S_2$ ($\pi-\pi^*$) transition. Reference compound **6** has an absorption peak at 353 nm due to metal-to-ligand charge transfer $S_0 \rightarrow {}^1\text{MLCT}$. **P-1** and **P-2** appear as two distinct bands in the absorption spectra. One band at shorter wavelengths is assigned to their localized $\pi-\pi^*$ transition, and the other band at longer wavelengths is attributed to intramolecular charge transfer (ICT) between Ru(II) bis(acetylide) complex or aryl diyne moieties as electron-rich donors and BODIPY moieties as electron-deficient acceptors. Compared with **M-1**, the absorption peak of **P-2** is red-shifted by 74 nm probably ascribing to the extended π -conjugation structure. Compared with **P-2**, **P-1** shows a 22 nm redshift for the absorption over 600 nm wavelength region. This could attribute to the introduction of the electron-rich Ru(II) complex moieties. Herein, the absorption spectra of **P-1** and **P-2** in the solid films appear more broad absorption bands in the range of 480–800 nm and obvious redshifts as high as 29 nm and 26 nm compared with those in solutions, respectively, which could be attributed to the strong interchain associations and aggregations. In addition, the optical bandgaps of **P-1** and **P-2** could be calculated as 1.52 and 1.73 eV from the thin film UV-vis spectra by using the equation $E_g = 1240/\lambda_{\text{edge}}$, demonstrating the tunable bandgaps upon the introduction of Ru(II) complex moieties in CP. In the fluorescence spectra [Fig. 1(b)] measured in solutions, **M-1** has an emission peak at 553 nm. The reference compound **6** has an emission peak at 403 nm. **P-2** has one emission peak at 645 nm which is obviously red-shifted relative to **M-1** due to the extended π -conjugation structure. When the Ru(II) complex moiety is introduced into the CP, **P-1** shows 8 nm redshift compared to **P-2**. We also found that the fluorescent emission intensities of both **P-1** and **P-2** in the solid films were too weak to be detected probably due to the aggregation-caused quenching (ACQ). In addition, the fluorescence decay profile of **P-1** was obtained with excitation at 580 nm and detection at 630 nm. The weight average lifetime (τ) of **P-1** was 1.02 ns (Supporting Information Fig. S19) which indicated the emission from singlet state. The small Stokes shift of **P-1** (19 nm) also indicated the emission from singlet state.⁴³ The optical data indicates that

TABLE 1 Optical Data of **6**, **M-1**, **P-1**, and **P-2** (1.0×10^{-5} mol L^{-1} , CH_2Cl_2)

	$\lambda_{\text{abs, sol.}}^{\text{a}}$ (nm) ^a	$\lambda_{\text{abs, film}}^{\text{b}}$ (nm) ^b	$\lambda_{\text{abs}}^{\text{a}}$ (nm) ^a	E_g (eV) ^c	Q_F^{d}
6	353	–	403	–	–
M-1	388, 538	–	553	–	0.64
P-1	375, 634	369, 663	653	1.52	0.08
P-2	409, 612	418, 638	645	1.73	0.26

^a Concentration of 10^{-5} mol L^{-1} in CH_2Cl_2 .

^b Drop coated from solutions on quartz substrates.

^c Optical band gaps were estimated from the absorption spectra in films by using the equation $E_g = 1240/\lambda_{\text{edge}}$.

^d Quantum yields were determined with ZnPc as fluorescence reference in DMF ($\Phi = 0.28$).⁴²

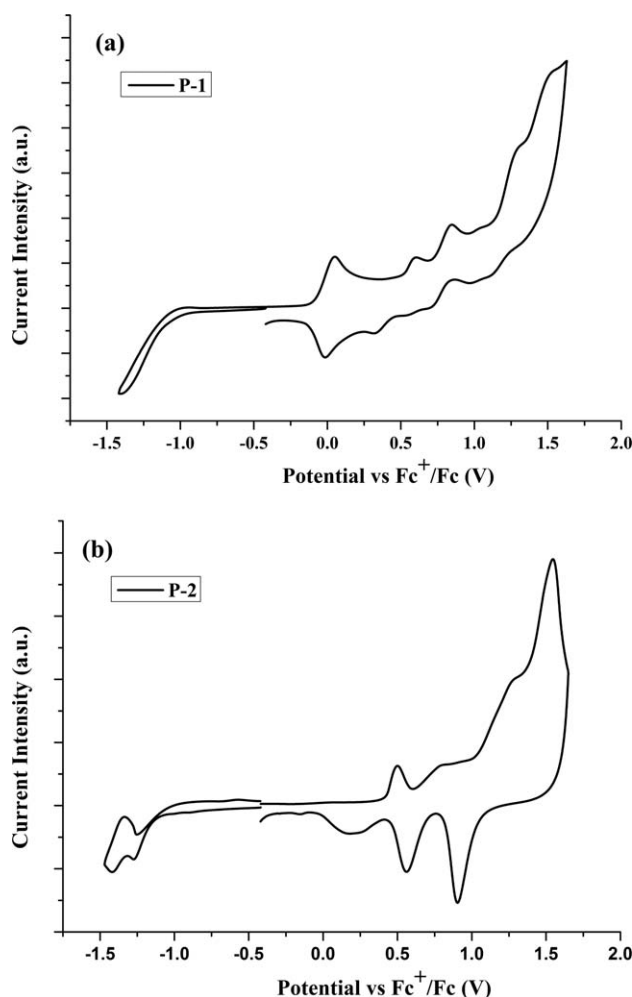


FIGURE 2 Cyclic voltammograms of **P-1** and **P-2**.

the introduction of Ru(II) complex into the main chain of the polymer could induce redshifts in both UV-vis absorption and fluorescence spectra.

Electrochemical Properties

The redox behaviors of the two polymers were measured by cyclic voltammetry (CV). Throughout, deoxygenated CH_2Cl_2 solutions and a scan rate of 50 mV s^{-1} were used. All measurements were performed in N_2 -saturated solutions containing 0.1 M tetrabutylammonium hexafluoro-

phosphate, and redox potentials were calibrated using a ferrocene-ferrocenium (Fc-Fc^+) redox couple as an external standard. A platinum wire was used as counter electrode and Ag/AgCl electrode was used as reference electrode. The CV curves of **P-1** and **P-2** are shown in Figure 2, and the electrochemical data is summarized in Table 2. As shown, **P-1** has one more redox wave with a small $E_{1/2} = 20 \text{ mV}$ ($\Delta E_p = 60 \text{ mV}$) [where $E_{1/2}$ represent the half-wave potential which get from $(E_{p,a} + E_{p,c})/2$; and δE_p means the separation of the peak potentials from $(E_{p,a} - E_{p,c})$] attributing to Ru(II)/Ru(III) redox process. This showed that the **P-1** could provide electrons easily than **P-2** due to the existence of Ru(II) complex. In their oxidation traces, the onset potentials of **P-1** and **P-2** occurred at -0.09 and $+0.43 \text{ V}$, respectively, probably arising from the oxidation of the electron-donor units. And in their reduction traces, **P-1** and **P-2** exhibited onset potentials at -0.96 and -1.08 V , which could be assigned to the reduction of the electron-acceptor BODIPY moiety. The highest occupied molecular orbital (HOMO) and lowest unoccupied molecular orbital (LUMO) energy levels of the polymers can be calculated according to the equations of $\text{HOMO} = -e(E_{\text{ox}}^{\text{onset}} + 4.8) \text{ (eV)}$ and $\text{LUMO} = -e(E_{\text{red}}^{\text{onset}} + 4.8) \text{ (eV)}$.⁴⁴ On the basis of these onset potentials, the HOMO/LUMO energy levels of **P-1** and **P-2** were determined to be $-4.71/-3.84 \text{ eV}$ and $-5.23/-3.72 \text{ eV}$ with the corresponding electrochemical bandgaps of 0.87 and 1.51 eV , respectively. The bandgap of **P-1** is 0.64 eV smaller than that of **P-2**, which demonstrates that the bandgaps of the CPs could be effectively decreased by introducing Ru(II) complexes into the polymer main chain.

Molecular Orbital Calculations

To gain a better insight into the geometric and electronic structure, we performed theoretical calculation analysis on the model Molecules **1** and **2** constituting the corresponding repeat units (Fig. 3). All calculations were performed at the B3LYP/(6-31G(d)+LanL2DZ) level by using Gaussian 09.^{30,45} Moreover, all the alkyl chains were replaced by methyl groups in the calculation for simplicity. Figure 3 displays the LUMO and HOMO of Model **1** and Model **2**. The calculated HOMO, LUMO, and the energy gaps (E_g) of the two models are listed in Table 2. As shown, the LUMO of both model compounds are mainly centered on the central BODIPY core, whereas the HOMO of Model **1** is mainly centered on Ru(II) complex unit and the HOMO of Model **2** is spread over the whole of

TABLE 2 Electrochemical Data of Polymers and Calculated HOMO, LUMO Energy Values

	From CV ^a					From Calculation		
	E _{onset ox} ^b (V)	HOMO (eV)	E _{onset red} ^b (V)	LUMO (eV)	E _g ^c (eV)	HOMO ^d (eV)	LUMO ^d (eV)	E _g ^{c,d} (eV)
P-1	-0.09	-4.71	-0.96	-3.84	0.87	-4.24	-2.48	1.76
P-2	0.43	-5.23	-1.08	-3.72	1.51	-4.88	-2.36	2.52

^a The ferrocene couple (Fc/Fc^+) was used as the internal reference and under our experimental conditions, $E(\text{Fc}^+/\text{Fc}) = 0.42 \text{ V}$ vs. Ag/AgCl .

^b E_{ox} and E_{red} were determined from the onset potentials of the oxidation and reduction waves.

^c $E_g = \text{LUMO} - \text{HOMO}$.

^d The data was from calculation of Model **1** and Model **2**.

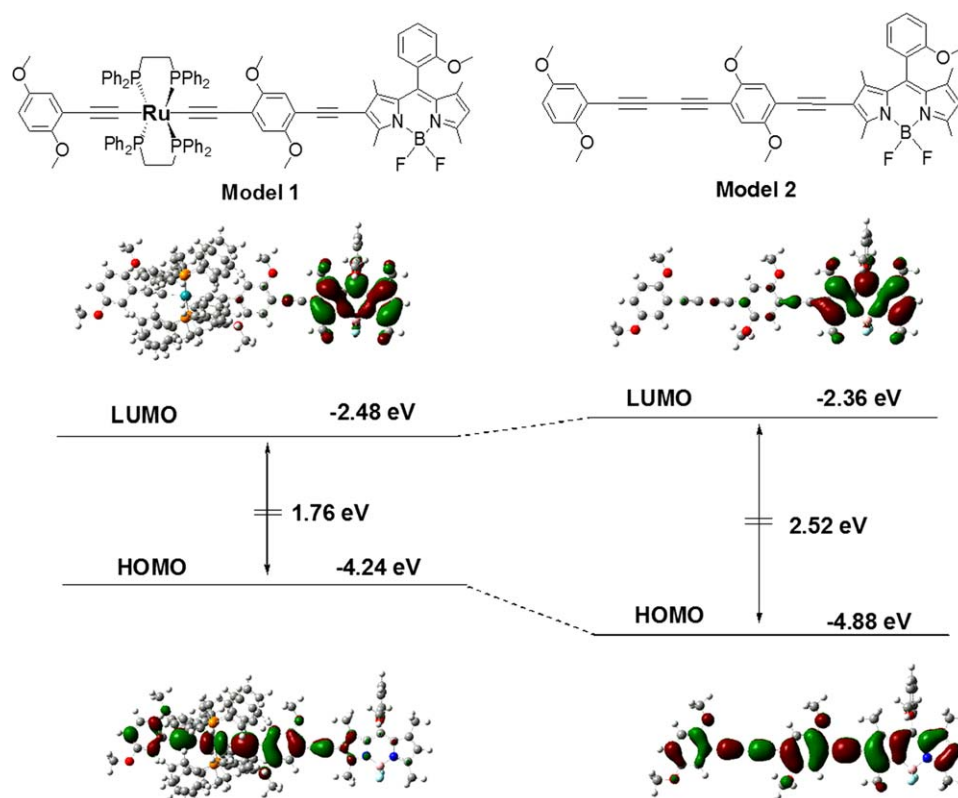


FIGURE 3 Structures and molecular orbital diagrams for LUMO and HOMO of designed model compounds **1**, and **2** from DFT calculations. [Color figure can be viewed in the online issue, which is available at wileyonlinelibrary.com.]

the conjugated backbone. Apparently, in comparison with Model **2**, Model **1** shows a higher HOMO level owing to the presence of the electron-rich Ru(II) complex moiety in the polymer backbone. Because of the strong donor–acceptor interaction between the Ru(II) complex and BODIPY unit, the calculated bandgap of Model **1** is 0.76 eV smaller than that of Model **2**. Although the calculated energy levels were higher than those determined by experiments, the trends in the bandgaps were in good agreement with the ones obtained by UV–vis and CV measurements of the polymers.

CONCLUSIONS

In summary, we have successfully synthesized a novel polymer **P-1** containing Ru(II) bis(acetylide) complex and BODIPY moieties in the main chain by Pd-catalyzed Sonogashira coupling reaction. The UV–vis absorption and fluorescence spectra indicate that the introduction of Ru(II) complex into the CP could significantly affect the optical properties of the polymer. Also, the optical, electrical, and calculated data further demonstrates a significant decreased bandgap of the polymer due to the introduction of Ru(II) complex. These photophysical and electrochemical properties indicate that the polymer might have potential in device-based applications.

ACKNOWLEDGMENTS

This work was supported by the National Natural Science Foundation of China (No. 51173078, 21174061, 21172106),

National Basic Research Program of China (2010CB923303) and open project of Beijing National Laboratory for Molecular Sciences.

REFERENCES AND NOTES

- 1 Y. J. Cheng, S. H. Yang, C. S. Hsu, *Chem. Rev.* **2009**, *109*, 5868–5923.
- 2 Q. Zhao, C. Huang, F. Li, *Chem. Soc. Rev.* **2011**, *40*, 2508–2524.
- 3 C. L. Ho, W. Y. Wong, *Coord. Chem. Rev.* **2011**, *255*, 2469–2502.
- 4 S. J. Liu, Y. Chen, W. J. Xu, Q. Zhao, W. Huang, *Macromol. Rapid Commun.* **2012**, *33*, 461–480.
- 5 G. R. Whittell, M. D. Hager, U. S. Schubert, I. Manners, *Nat. Mater.* **2011**, *10*, 176–188.
- 6 A. Wild, A. Teichler, C. L. Ho, X. Z. Wang, H. M. Zhan, F. Schlütter, *J. Mater. Chem. C*, **2013**, *1*, 1812–1822.
- 7 B. Happ, A. Winter, M. D. Hager, U. S. Schubert. *Chem. Soc. Rev.* **2012**, *41*, 2222–2255.
- 8 N. R. Evans, L. Sudha, C. S. K. Mak, S. E. Watkins, S. I. Pascu, A. Kohler, *J. Am. Chem. Soc.* **2006**, *128*, 6647–6656.
- 9 A. Kimyonok, B. Domercq, A. Haldi, J. Y. Cho, J. R. Carlise, X. Y. Wang, *Chem. Mater.* **2007**, *19*, 5602–5608.
- 10 C. T. Wong, W. K. Chan, *Adv. Mater.* **1999**, *11*, 455–459.
- 11 P. Nguyen, P. Gomez-Eliphe, I. Manners, *Chem. Rev.* **1999**, *99*, 1515–1548.

- 12 G. J. Zhou, W. Y. Wong, *Chem. Soc. Rev.* **2011**, *40*, 2541–2566.
- 13 K. A. Williams, A. J. Boydston, C. W. Bielawski, *Chem. Soc. Rev.* **2007**, *36*, 729–744.
- 14 W. Y. Wong, X. Z. Wang, Z. He, A. B. Djuricic, C. T. Yip, K. Y. Cheung, *Nat. Mater.* **2007**, *6*, 521–527.
- 15 X. Y. Wang, C. Avendaño, K. R. Dunbar, *Chem. Soc. Rev.* **2011**, *40*, 3213–3238.
- 16 Y. Chi, P. T. Chou, *Chem. Soc. Rev.* **2010**, *39*, 638–655.
- 17 Z. P. Liu, W. J. He, Z. J. Guo, *Chem. Soc. Rev.* **2013**, *42*, 1568–1600.
- 18 V. Marin, E. Holder, R. Hoogenbooma, U. S. Schubert, *Chem. Soc. Rev.* **2007**, *36*, 618–635.
- 19 W. L. Leong, J. J. Vittal, *Chem. Rev.* **2011**, *111*, 688–764.
- 20 A. Loudet, K. Burgess, *Chem. Rev.* **2007**, *107*, 4891–4932.
- 21 R. Gresser, M. Hummert, H. Hartmann, K. Leo, M. Riede, *Chem.—Eur. J.* **2011**, *17*, 2939–2947.
- 22 R. Guliyev, S. Ozturk, Z. Kostereli, E. U. Akkaya, *Angew. Chem. Int. Ed.* **2011**, *50*, 9826–9831.
- 23 S. Kolemen, O. A. Bozdemir, Y. Cakmak, E. U. Akkaya, *Chem. Sci.* **2011**, *2*, 949–954.
- 24 L. T. Zeng, C. J. Jiao, X. B. Huang, K. W. Huang, W. S. Chin, J. S. Wu, *Org. Lett.* **2011**, *13*, 6026–6029.
- 25 F. Jakle, *Chem. Rev.* **2010**, *110*, 3985–4022.
- 26 K. Tanaka, Y. Chujo, *Macromol. Rapid Commun.* **2012**, *33*, 1235–1255.
- 27 S. L. Zhu, J. T. Zhang, J. Janjanam, G. Vegesna, F. T. Luo, A. Tiwari, *J. Mater. Chem. B*, **2013**, *1*, 1722–1728.
- 28 S. L. Zhu, N. Dorh, J. T. Zhang, G. Vegesna, H. H. Li, F. T. Luo, *J. Mater. Chem.* **2012**, *22*, 2781–2790.
- 29 W. H. Wu, J. Z. Zhao, J. F. Sun, L. Huang, X. Y. Yi, *J. Mater. Chem. C*, **2013**, *1*, 705–716.
- 30 W. H. Wu, J. Z. Zhao, H. M. Guo, J. F. Sun, S. M. Ji, Z. L. Wang, *Chem.—Eur. J.* **2012**, *18*, 1961–1968.
- 31 T. Zhang, X. J. Zhu, W. K. Wong, H. L. Tam, W. Y. Wong, *Chem.—Eur. J.* **2013**, *19*, 739–748.
- 32 Y. Gabe, Y. Urano, K. Kikuchi, H. Kojima, T. Nagano, *J. Am. Chem. Soc.* **2004**, *126*, 3357–3367.
- 33 Y. Z. Wu, X. Ma, J. M. Jiao, Y. X. Cheng, C. J. Zhu, *Synletters* **2012**, *23*, 778–782.
- 34 J. Chatt, R. G. Hayter, *J. Chem. Soc.* **1961**, 896–904.
- 35 M. A. Fox, J. E. Harris, S. Heider, V. P. Gregorio, M. E. Zakrzewka, J. D. Farmer, *J. Organomet. Chem.* **2009**, *694*, 2350–2358.
- 36 Y. Z. Wu, Y. Dong, J. F. Li, X. B. Huang, Y. X. Cheng, C. J. Zhu, *Chem. Asian J.* **2011**, *6*, 2725–2729.
- 37 G. Castruita, E. Arias, I. Moggio, F. Pérez, D. Medellín, R. Torres, *J. Mol. Struct.* **2009**, *936*, 177–182.
- 38 A. Klein, O. Lavastre, J. Fiedler, *Organometallics* **2006**, *25*, 635–643.
- 39 D. Touchard, C. Morice, V. Cadierno, P. Haquette, L. Toupet, P. H. Dixneuf, *J. Chem. Soc. Chem. Commun.* **1994**, *7*, 859–860.
- 40 A. S. Hay, *J. Org. Chem.* **1962**, *27*, 3320–3321.
- 41 S. L. Zhang, X. Y. Liu, T. Q. Wang, *Adv. Synth. Catal.* **2011**, *353*, 1463–1466.
- 42 H. He, P. C. Lo, S. L. Yeung, W. P. Fong, D. K. P. Ng, *Chem. Commun.* **2011**, *47*, 4748–4750.
- 43 S. W. Thomas, S. Yagi, T. M. Swager, *J. Mater. Chem.* **2005**, *15*, 2829–2835.
- 44 C. C. Ho, Y. C. Liu, S. H. Lin, W. F. Su, *Macromolecules* **2012**, *45*, 813–820.
- 45 R. D. Costa, J. Arago, E. Orti, T. M. Pappenfus, K. R. Mann, K. Matczyszyn, M. Samoc, J. L. Zafra, J. T. L. Navarrete, J. Casdo, *Chem.—Eur. J.* **2013**, *19*, 1476–1488.